SECOND EUROPEAN CONFERENCE ON EARTHQUAKE ENGINEERING
AND SEISMOLOGY, ISTANBUL AUG. 25-29, 2014

INVESTIGATING THE IN-PLANE MECHANICAL BEHAVIOR OF URM PIERS VIA DSFM

Shenghan ZHANG[1], Sarah PETRY[2] and Katrin BEYER[3]

ABSTRACT

In this paper we use the novel Disturbed Stress Field Model (DSFM) from Facconi et al. (2013) to model the lateral in-plane behaviour of different unreinforced masonry (URM) walls which we tested at the laboratory of the EPF Lausanne, Switzerland. The model uses the failure criterion developed by Ganz (1985) for URM and is implemented in the software VecTor 2.

In the first part of this article, we show that the DSFM gives good estimates for the initial stiffness of the walls but underestimates the displacement and force capacity of our URM walls. This is due to the confinement of the mortar base joint which is confined by the wall foundation. However, we show that this phenomenon can be accounted for by replacing the compression strength of the masonry of the first brick layer by the strength of the brick itself.

Using this improved model, we compare the numerical results to the experimental results with regard to displacements and strains. We show that the simplification of the masonry to a continuous material is correct when comparing the global engineering demand parameters (EDPs), e.g., force-displacement behaviour of the walls or crack pattern. However, when comparing local EDPs, e.g., strains and crack widths, significant differences can be obtained. These differences are mainly caused by the torque of the bricks inside the walls (Mann and Müller, 1982). We show that this distortion gets less important with increasing shear span and that for a wall with higher shear span the assumption of a continuous material gives reasonable results even at the local level.

INTRODUCTION

In recent decades different methods have been developed for simulating the non-linear behaviour of unreinforced masonry (URM) components. Among these methods are simplified micro models (e.g., Lourenço, 1996; Snozzi and Molinari, 2013), smeared crack models (e.g., Gambarotta and Lagomarsino, 1997) or damage models (e.g., Pelà et al., 2013). Although these models link local

[1] Shenghan Zhang, Earthquake Engineering and Structural Dynamics (EESD), School of Architectural, Civil and Environmental Engineering (ENAC), École Polytechnique Fédérale de Lausanne (EPFL), Shenghan.zhang@epfl.ch
[2] Sarah Petry, Earthquake Engineering and Structural Dynamics (EESD), School of Architectural, Civil and Environmental Engineering (ENAC), École Polytechnique Fédérale de Lausanne (EPFL), sarah.petry@epfl.ch
[3] Katrin Beyer, Earthquake Engineering and Structural Dynamics (EESD), School of Architectural, Civil and Environmental Engineering (ENAC), École Polytechnique Fédérale de Lausanne (EPFL), katrin.beyer@epfl.ch

to global engineering demand parameters (EDPs), e.g., local strain limits to the global ultimate displacement capacity, all these models have only been compared to experimental results at the global level. This was largely due to the absence of experimental campaigns that documented local deformation measures of masonry walls such as strains in bricks and crack widths in joints. To overcome this lack of data, we tested a set of six URM walls under quasi-static cyclic in-plane loading (Petry and Beyer, 2013, 2014a). An optical measurement system allowed us measuring strains in bricks and relative displacements between the bricks. Thus, we were able to collect data on the local behaviour of URM walls which we use currently for developing a mechanical model for predicting the displacement capacity of URM walls.

In this paper we use the results of these EPFL tests to validate a newly published model for the prediction of the nonlinear behaviour of URM structures. Based on the Disturbed Stress Field Model (DSFM), a phenomenological macro model for masonry is recently put forward by Facconi et al. (2013). The model is based on the failure criterion for URM by Ganz (1985) and implemented in the software VecTor 2 (Wong et al., 2013). Compared with conventional smeared crack models, DSFM is able to combine the average macroscopic representation of the material behaviour with the local shear stress shear slip response of mortar joints (Facconi et al., 2013). In this article, we show that the prediction of the force-displacement curve of masonry walls using DSFM can be further improved by implementing some findings, which we derived from test observations when developing the mechanical model for the displacement capacity (Petry and Beyer, 2014b). In addition, we provide a first comparison of the results comparing the global and local EDPs. We show that the model is able to give reasonable estimates also at the local deformation level, as long as the shear solicitation in the wall is limited and the torque of the bricks (Mann and Müller, 1982) is not too important.

EXPERIMENTAL CAMPAIGN USED FOR COMPARISON

In order to investigate the influence of the boundary conditions on URM walls, we tested a series of six identical URM walls at the structural laboratory of the EPF Lausanne. All walls had the same dimensions (L x H x T = 2.01 m x 2.25 m x 0.20 m) and the tests varied by means of the applied boundary conditions. Hence, the different walls were subjected to axial stress ratios σ_0/f_u of 0.09, 0.18 or 0.26 respectively, and shear span ratios H_0/H of 0.5, 0.75 or 1.5, where σ_0 is the mean axial stress, and f_u the compression strength of the masonry and H_0 is the shear span (see Table 1). More information on the test series can be found in Petry and Beyer (2014a) and the entire data set is also publically available (2013).

During testing, we tracked with a set of cameras the displacement of four LEDs on each full brick of the masonry walls. Therefore, we were able to determine local deformation measures such as average strains in the bricks and deformations in the joints. The LEDs can be seen as black dots on the wall in Fig. 1.

Table 1. Boundary conditions of PUP1-5 (Petry and Beyer, 2014a)

Specimen	Normal stress level	Axial stress σ_0	Degree of coupling	Shear span H_0	Failure mode
PUP1	Intermediate	0.18 f_u	Strong	0.5H	Diagonal shear
PUP2	Intermediate	0.18 f_u	Strong	0.75H	Diagonal shear
PUP3	Intermediate	0.18 f_u	Intermediate	1.5H	Flexural rocking
PUP4	High	0.26 f_u	Intermediate	1.5H	Hybrid
PUP5	Low	0.09 f_u	Strong	0.75H	Diagonal shear

Figure 1. Photo of EPFL test stand (Petry and Beyer, 2014a)

MASONRY MODEL IMPLEMENTED IN VECTOR 2

All wall analyses presented in this paper are performed using the Disturbed Stress Field Model (DSFM) by Facconi et al. (2013) implemented in VecTor 2. This method is based on a one-dimensional stress-strain relationship in the direction of the principle compression strut. The influence of the stress perpendicular to this compression strut and the anisotropy of the masonry are considered by modification of the maximum strength according to Ganz (1985). Facconi et al. (2013) further considered the compression softening effect by applying a reduction factor to the ultimate compression strength. The increased flexibility parallel to the bed joints is accounted for by considering an additional strain in this direction (based on Mohr-Coulomb friction law).

The material parameters used for the numerical simulation in VecTor 2 are listed in Table 2. Note that some of the parameters could not be obtained from the material tests performed in Petry and Beyer (2013). The missing parameters were therefore estimated and the source of all parameters is indicated in Table 2. In order to simulate the same boundary conditions as for the experiments (see Table 1), the vertical load and lateral displacement was applied to the models by means of a rigid body connected to the top of the wall. Hence, the axial load was applied in form of a uniform stress applied through the rigid body onto the wall and was maintained constant throughout the pushover analysis. The shear span was controlled by the position of the imposed displacement on the rigid body.

In order to investigate the ability of the DSFM (Facconi et al., 2013) to predict the behaviour of URM walls, we compare in the following the numerical results with the experiments using global and local EDPs. Hence, at first the numerical and experimental results are compared at the global level on

the basis of the force-displacement response and the crack pattern. Then we compare local EDPs in form of vertical and shear strains at two different drift levels in the pre peak branch for one wall developing a typical diagonal shear failure mode and for one wall developing a flexural mode. In a last step, we use the strains in order to obtain the curvature and shear strain profiles. Based on these, we compute the shear and flexural displacements and compare these again to the total displacement profiles of the walls.

Table 2. Materials and geometrical properties for DSFM

f_{my} = 5.87 MPa *	E_{my} = 3550 MPa *
$f_{mx} = f_{my} \times 0.3$ †	$E_{mx} = 1000 \times f_{mx}$ †
f_{ty} = 0.5 MPa *	G_f^I = 0.1 MPa ‡
f_{tx} = 0.05 MPa ↿	ε_0 =3.0 mm/m ‡
c = 0.27 MPa *	t_{hj} = 300 mm *
tan_ϕ = 0.94 *	t_{bj} = 190 mm *
μ = 1 ‡	s_{hj} = 11 mm *
v_{xy} = 0.2 *	s_{bj} = 11 mm *

* Parameters taken from Petry and Beyer (2013)
† Parameters taken from SIA (2005)
‡ Parameters taken from the second example in Facconi et al. (2013)
↿ Parameters set to default values in VecTor 2 (Version 3.7)

COMPARISON OF GLOBAL EDPs – FORCE-DISPLACEMENT RELATIONSHIP AND CRACK PATTERN

In Fig. 2, the force-displacement relationship obtained from the pushover analysis in Vector 2 (conitnuous black line) is compared with the force-displacement hysteresis obtained from the different walls. In order to compare numerical and experimental results in the positive and negative direction of the wall, the same pushover analysis is plotted once for the positive and once fore the negative loading directions. It can be seen that the numerical model underestimates the displacement and force capacity significantly for four out of the five analysed walls, i.e., PUP2-5. However, the model predicts correctly the failure mechanism for all walls apart from PUP5. In this case VecTor 2 predicts a flexural rocking failure while a diagonal shear failure was observed during testing (see Table 1).

In Petry and Beyer (2014b) it is concluded that the strength of the bottom brick layer of the walls must be considerably higher than the masonry strength obtained from compression tests on masonry wallets. The walls were all built on steel plates which were then clamped to a concrete foundation (see Fig.1). These foundation confines the mortar layer at base and hinders it thus to expand. Normally, compression failure in masonry is provoked by tensile failure of the bricks at the brick-mortar interface, because the different Poisson's ratio of the brick and the mortar causes them to expand differently. However, because of the confined mortar joint at the base, this tensile failure of the bottom brick is hindered and the critical section for a typical compression failure is not the base joint but the first joint above th base (Petry and Beyer, 2014b). In order to account for this in the numerical model, we replaced thus the masonry strength of the first brick layer by the compression strength of the brick $f_{my} = f_{B,c}$ = 35 MPa.

The comparison of the simulation results between the modified model (VecTor 2 (M)) and the original model (VecTor 2) are shown in Fig. 2. It can be seen that especially for the walls PUP3-5, where flexural deformations prevailed, the implementation of the increased compression strength in the bottom brick layer improved the results remarkably. The effect is particularly significant for walls developing a flexural mechanism, since the non-linear displacements result mainly from the reduced size of the compression zone. However, the more the effective area reduces, the more the stresses in the toe increase and the reduction of the effective area is therefore limited by the compression strength at the base. In the case of diagonal shear failure, the capacity is dominated by the capacity along the entire diagonal. Thus, for these walls the influence of the strength in the bottom layer plays not such an important role, while it has an important influence on the walls developing a significant flexural mode, e.g., PUP3-5. Note that when we considered the increased masonry strength in the lower

masonry layer the prevailing failing mechanism for PUP5 showed signs of the onset of a diagonal shear failure, which was the failure mechanism we observed during testing (see Table 2).

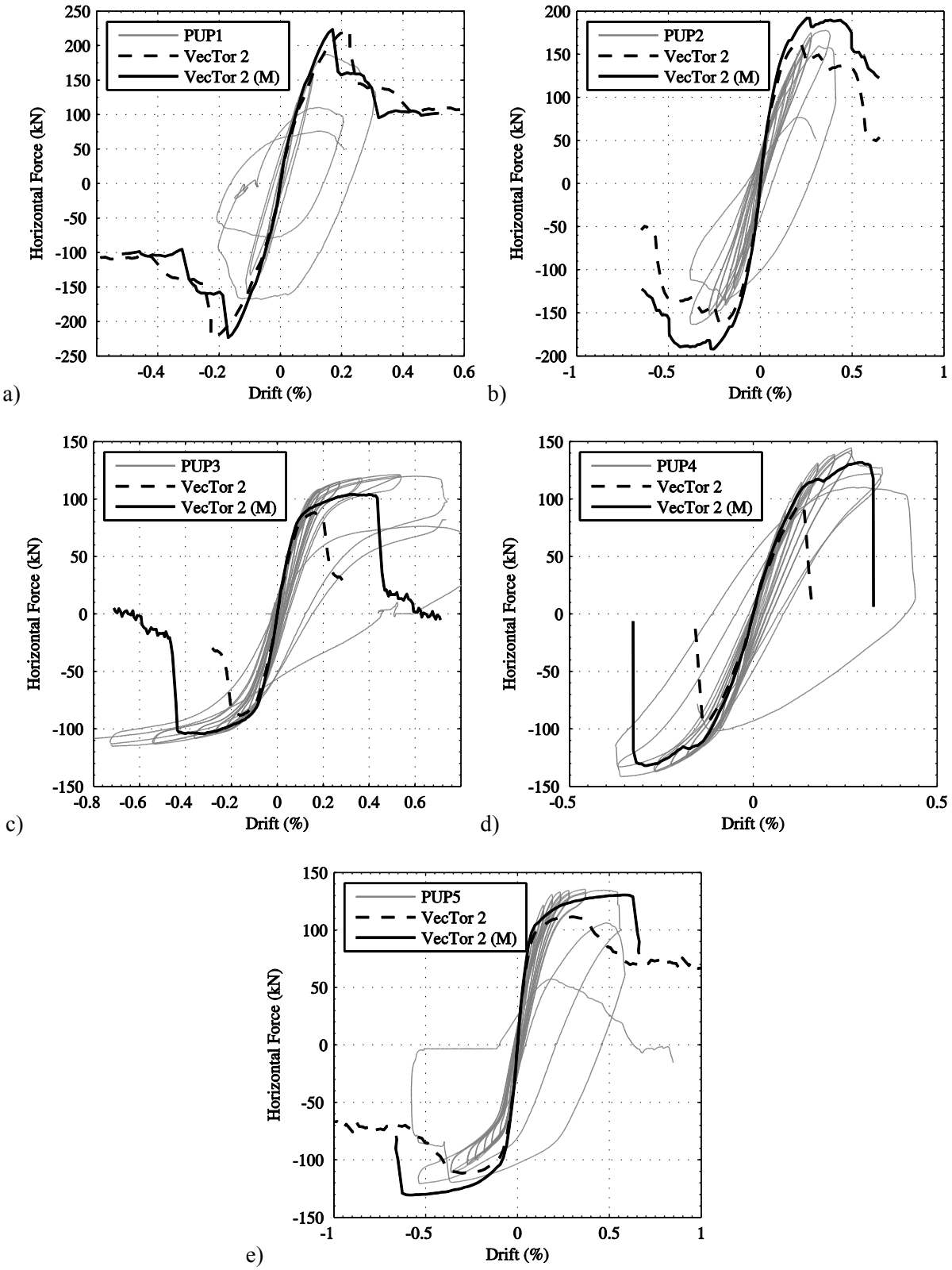

Figure 2. Comparison of the global force-displacement response obtained with Vector 2, once without and once with considering the confinement of the mortar joint in base for the first five walls of the PUP-series

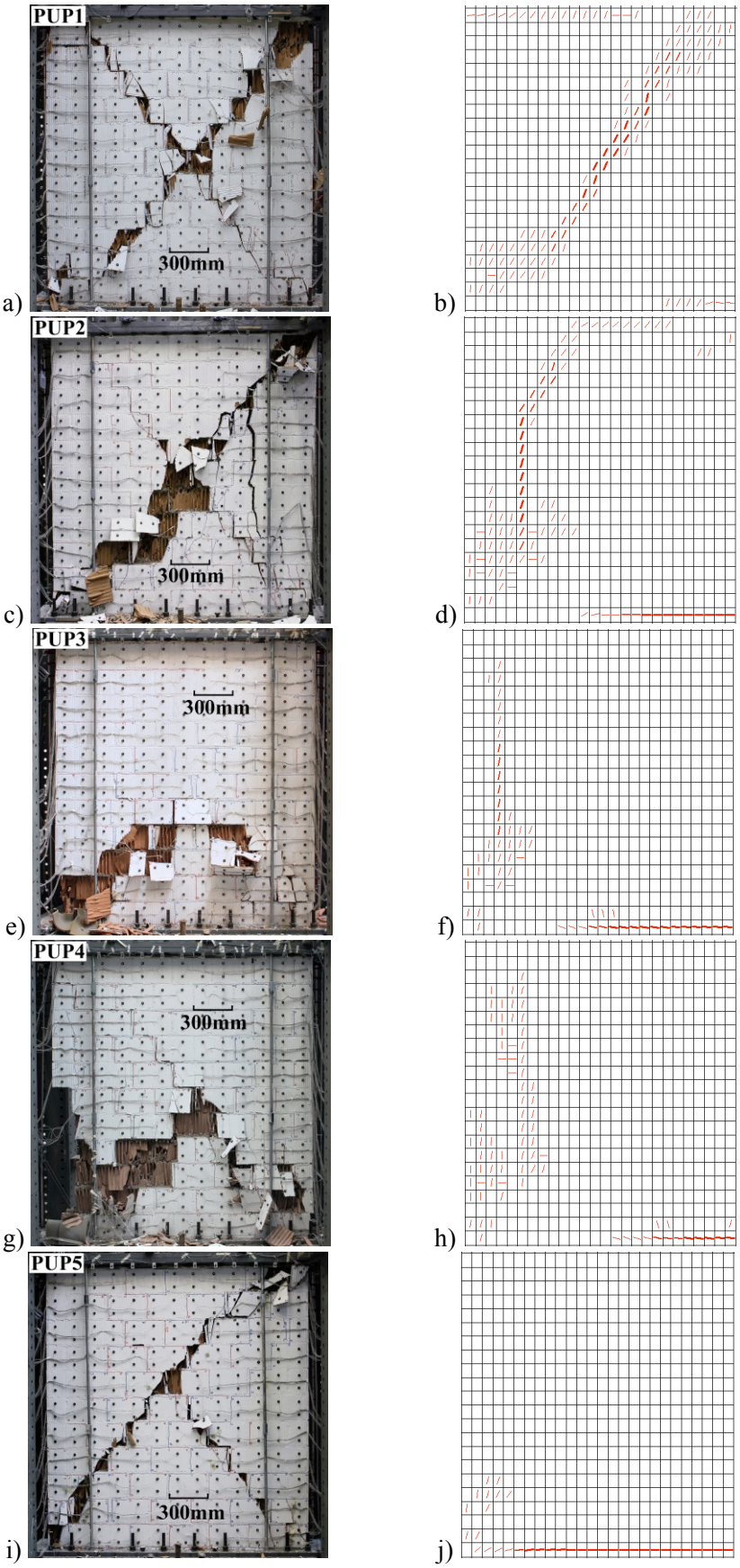

Figure 3. Comparison of the crack pattern from experiments after axial load failure (Petry and Beyer, 2013) and the damage (red lines) as indicated by Vector 2 (Wong et al., 2013) immediately after obtaining the lateral peak force for the modified model (VecTor 2 (M)).

In Fig. 3 we compare the crack pattern obtained with the modified model in Vector 2 (VecTor 2 (M)) with a photo of each test unit after the walls could not sustain the axial load any longer. PUP1 was tested with fixed-fixed boundary conditions with a shear span of approximately 0.5 the wall height and it can be seen that crack pattern in the model corresponds well to the cracks observed for PUP1. In the case of PUP2 and PUP5 a limited rotation was allowed at the top of the wall. This was done by controlling the shear span constant at 0.75 times the wall height. However, for both the walls, Petry and Beyer (2014a) observed that first diagonal cracks which developed in these walls were indeed more vertical than the crack which can be seen in the photos after axial load failure (see Figs. 3.c and 3.i). The inclination of the first developing shear crack was hence quite similar to the one indicated by the numerical simulation (see Figs. 3.d and 3.j). Only shortly before the peak strength was attained, the orientation of the cracks changed and followed the geometrical diagonal as shown in the photos of Figs. 3.c and 3.i. We concluded therefore that the improved numerical model can be used for localizing the developing cracks before peak strength is obtained. In the case of PUP3 and PUP4 an flexural mode and hybrid mode was observed and in both cases it can be seen that crack pattern corresponds well to the one observed during experiments.

COMPARISON OF LOCAL EDPs – VERTICAL AND SHEAR STRAINS

In the previous section we showed that the model gives good estimates for the global EDPs when considering the increased strength in the bottom brick row. However, in order to get a better feeling for the suitability of the use of local strain limits for determining the global displacement capacity, we were interested in comparing also local EDPs. Therefore, in this section, we analyse the strains for the two walls PUP1 and PUP3. These two tests units are chosen because they developed a clear diagonal shear failure and rocking failure, respectively. The strains are shown for the two drift limits before peak strength is obtained. The strains from experiments are estimated using the relative displacement developing between two rows of bricks. They represent thus the average deformations which developed over one mortar joint and one brick. The approach used for determining the experimental strains is explained in more detail in Petry and Beyer (2014c). In order to compare directly the strains from the experiments with the numerical results from Vector 2 (Wong et al., 2013), the mesh in the numerical model was defined such that one brick was modelled by 2 x 4 elements. Hence, the strains from the numerical results were determined in the same manner as the experimental results, using always the nodal displacement which corresponded to the same position as the equivalent LED on the wall.

Detailed comparison of the numerical and experimental strains shows that the strains are generally better estimated for the wall developing a flexural mechanism (PUP3) than the wall developing a diagonal shear mechanism (PUP1). In the case of PUP1, it can be seen that the vertical strain ε_{yy} obtained from the expriments (PUP1, see Figs. 4.a and 4.c) show some significant alteration which is not visible in the vertical strains obtained from the numerical model. This alteration of vertical stresses is caused by a phenomenon first described by Mann and Müller (1982). They observed that the shear stresses provoke the bricks to rotate and creates thus a partial uplift between the bricks. This partial uplift is well visible through positive vertical strains in the experimental results (see Figs. 4.a and 4.c). However, in the case of the numerical model, the bricks and mortar are modelled as one continuous material and this phenomenon cannot be reproduced. In addition, this partial uplift of the bricks causes the masonry to form a typical stair step diagonal crack and in Figs. 4.b and 4.d it can be seen that for the experimental results significant shear strains γ_{xy} concentrate along this crack.

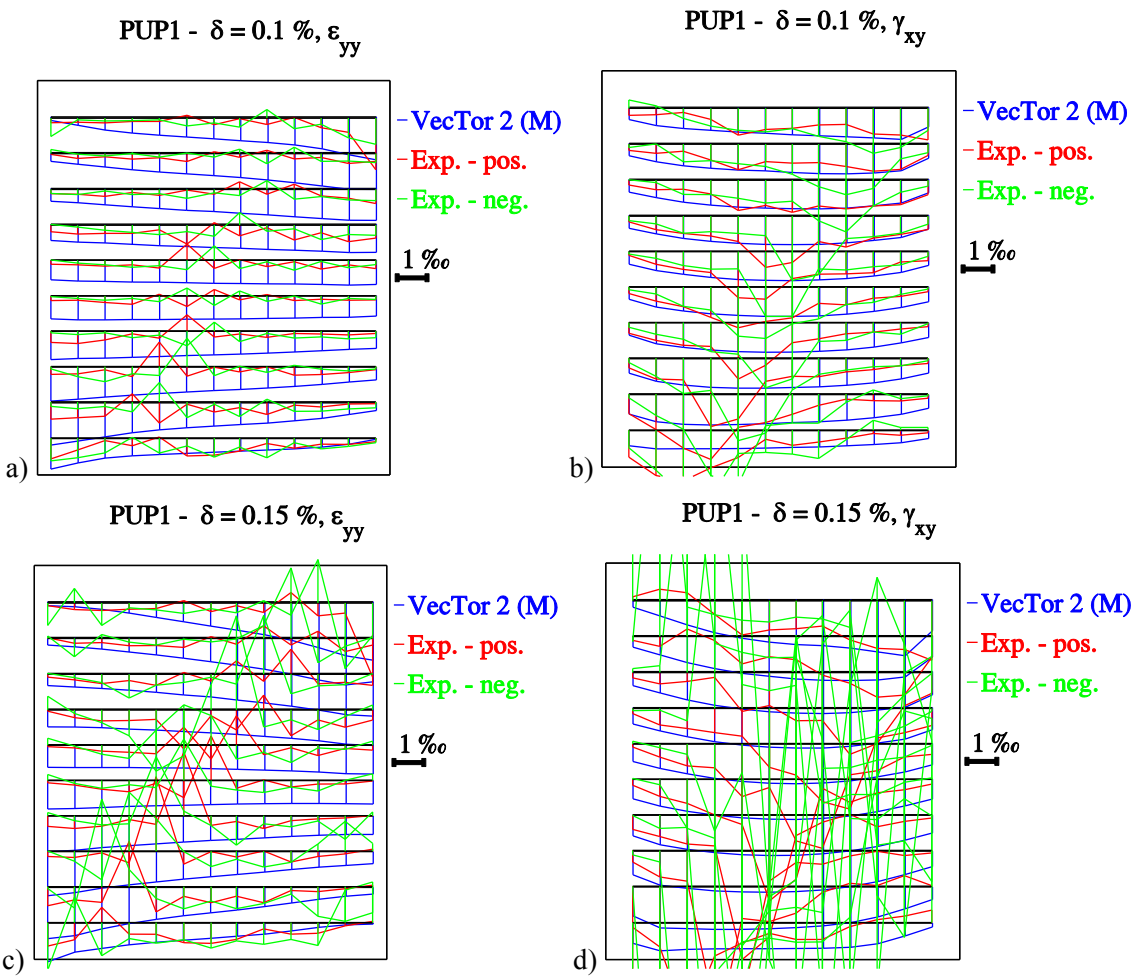

Figure 4. Comparison of vertical strains ε_{yy} and shear strains γ_{xy} for a wall showing a typical diagonal shear failure (PUP1) when reaching the first time the drifts (a,b) 0.1% and (c,d) 0.15 %

In the case of PUP3, generally a good agreement between the vertical strains ε_{yy} from the experiments and the numerical analysis can be found. For instance, the area in compression is similar for the experimental strains as well as for the numerical strains (see Figs. 5.a and 5.c). However, the comparison of the numerically and experimentally determined shear strains γ_{xy} is less satisfactory than the case for the vertical strains ε_{yy}. First, the shear strains obtained with the numerical simulation are significantly higher than the shear strains obtained from the experiments. In addition, it can be observed that when the compressed area increases with increasing height of the wall, the shear strain obtained through the numerical simulation do not distribute equally over the whole compressed zone (see Figs. 5.b and 5.d), as it is the case for the experimental results. In addition, it can be observed that the shear strains in VecTor 2 are underestimated for small compressed zone and overestimated when the whole section is in compression.

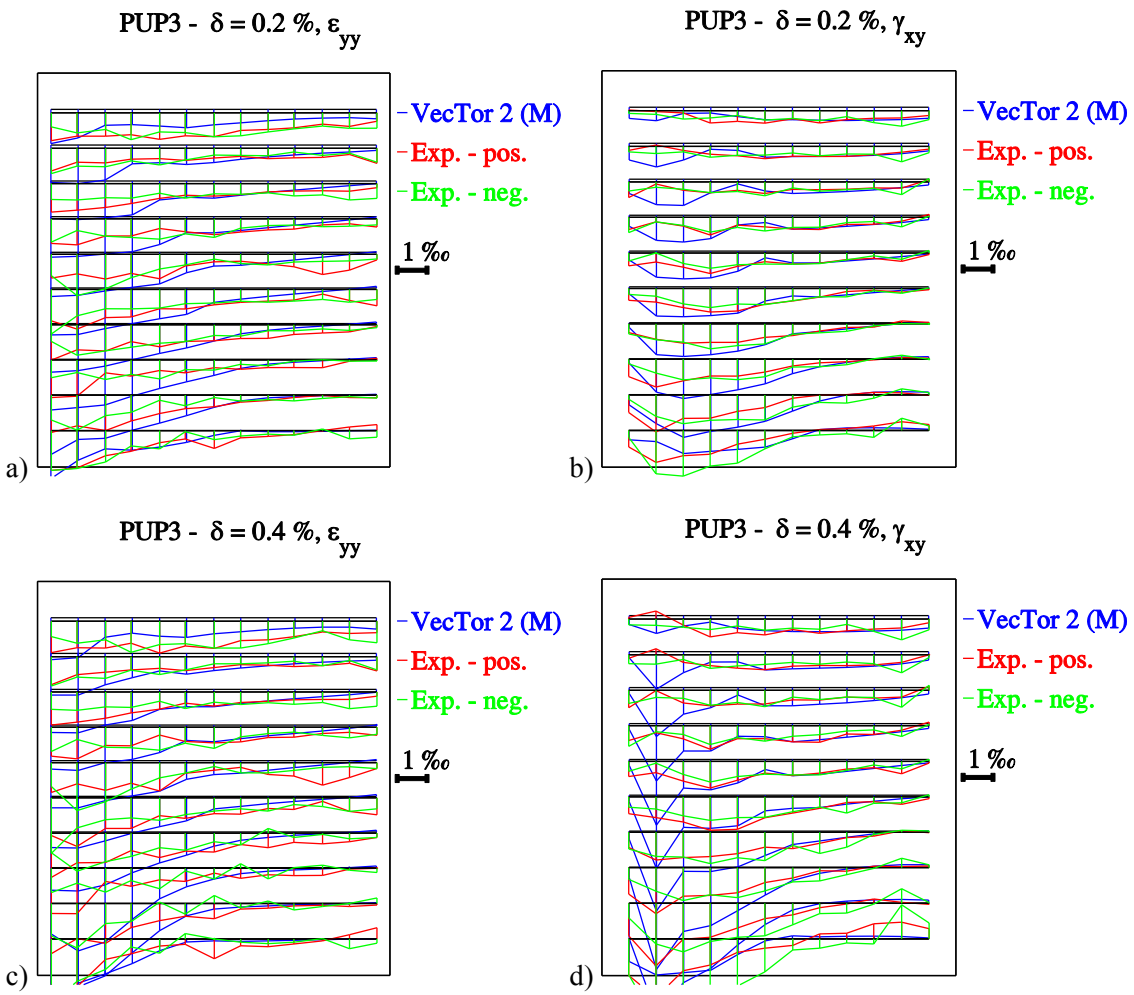

Figure 5. Comparison of vertical strains ε_{yy} and shear strains γ_{xy} for a wall showing a typical flexural rocking failure (PUP3) when reaching the first time the drifts (a,b) 0.2% and (c,d) 0.4 %

COMPARISON OF THE DEFORMATION QUANTITIES DUE TO SHEAR AND FLEXURAL SOLICITATIONS

Assuming a plane-remaining section, the displacement due to shear and flexural deformation can be computed by integration of the curvature and the shear strain. The curvature and shear strains are computed using the strains shown in Figs. 4 and 5, but with considering only the strains of the compressed portion of the walls. For the experimental results, the curvature and shear strain could only be obtained from the deformations between two rows of bricks. Hence, in order to account for the rotation which takes place through opening of the base joint, the rotation of the lower brick row is estimated from the vertical displacement of the bottom bricks located in the compressed zone and added to the initial rotation (see offset of the rotation profile at height of the first brick layer in Figs. 6 and 7).

When the axial load was applied to PUP3, the wall behaved not symmetrically and developed a significant lateral displacement even though only vertical loads were applied. When applying the lateral displacement, this was always applied with respect of the displacement obtained after axial load application(see also Fig. 2), while in Figs. 4 to 7 the deformations are always computed with respect to the measurement done before the axial load application. Therefore, significant differences between the positive and negative loading direction can be observed for PUP3 and when comparing the experimental results with the numerical results it is suggested using the average of both loading directions.

PUP1 was subjected to fixed-fixed boundary which resulted thus in a shear span of aproximately 0.5 *H*. Due to the short shear span, few flexural deformations form and the total displacement develop mainly through shear deformations (see Fig. 6). In Fig. 4 we noticed that the DSFM tends to overestimate the vertical strains of PUP1 when compared to the strains obtained from experiments. In Fig. 6, it can be seen that this overestimation of the flexural deformations is compensated through a significant opening of the bottom joint (reflected through the significant rotation measured in the bottom brick). The DSFM simplifies the masonry to a continuous material. However, in reality the masonry is composed of relatively rigid bricks in combination with soft mortar joints and the short shear span in PUP1 forces the brick to rotate (Mann and Müller, 1982). Thus, brick and mortar start to disintegrate and the assumption of a continuous material does not hold any longer at the local level. Nevertheless, the different displacement components obtained with the numerical modelling match good with the experimental results (see Fig. 6).

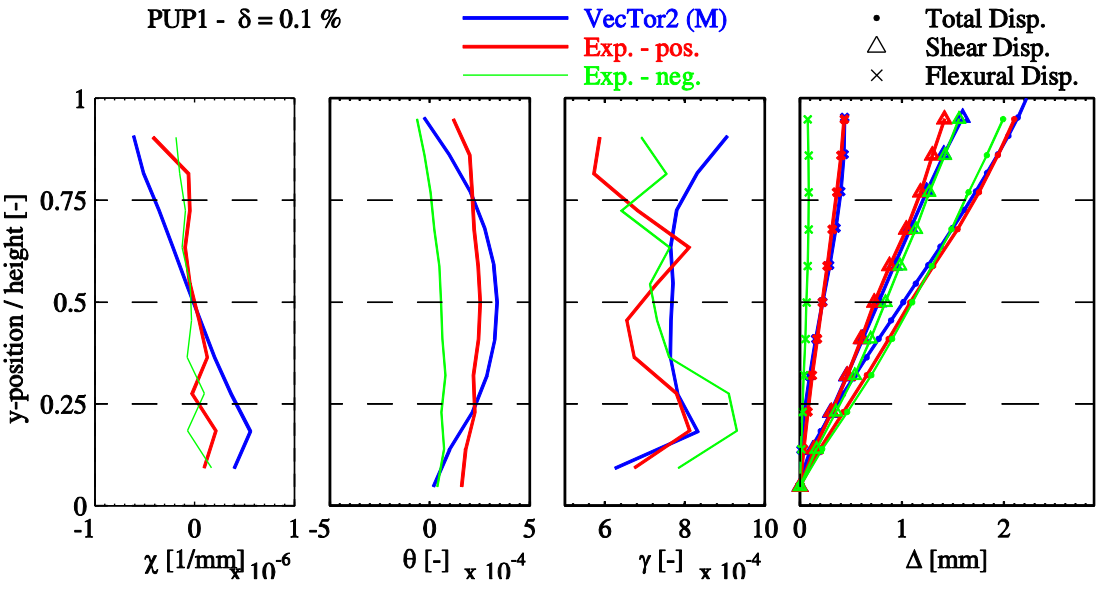

a)

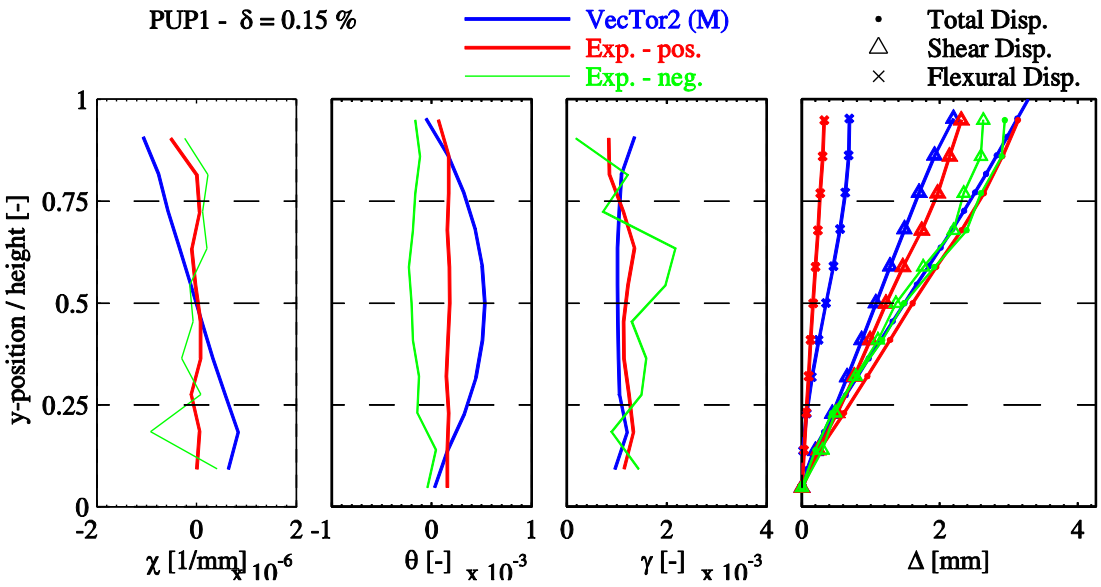

b)

Figure 6. Comparison of deformation quantities of PUP1 for different drifts (a) 0.1 % and (b) 0.15 %

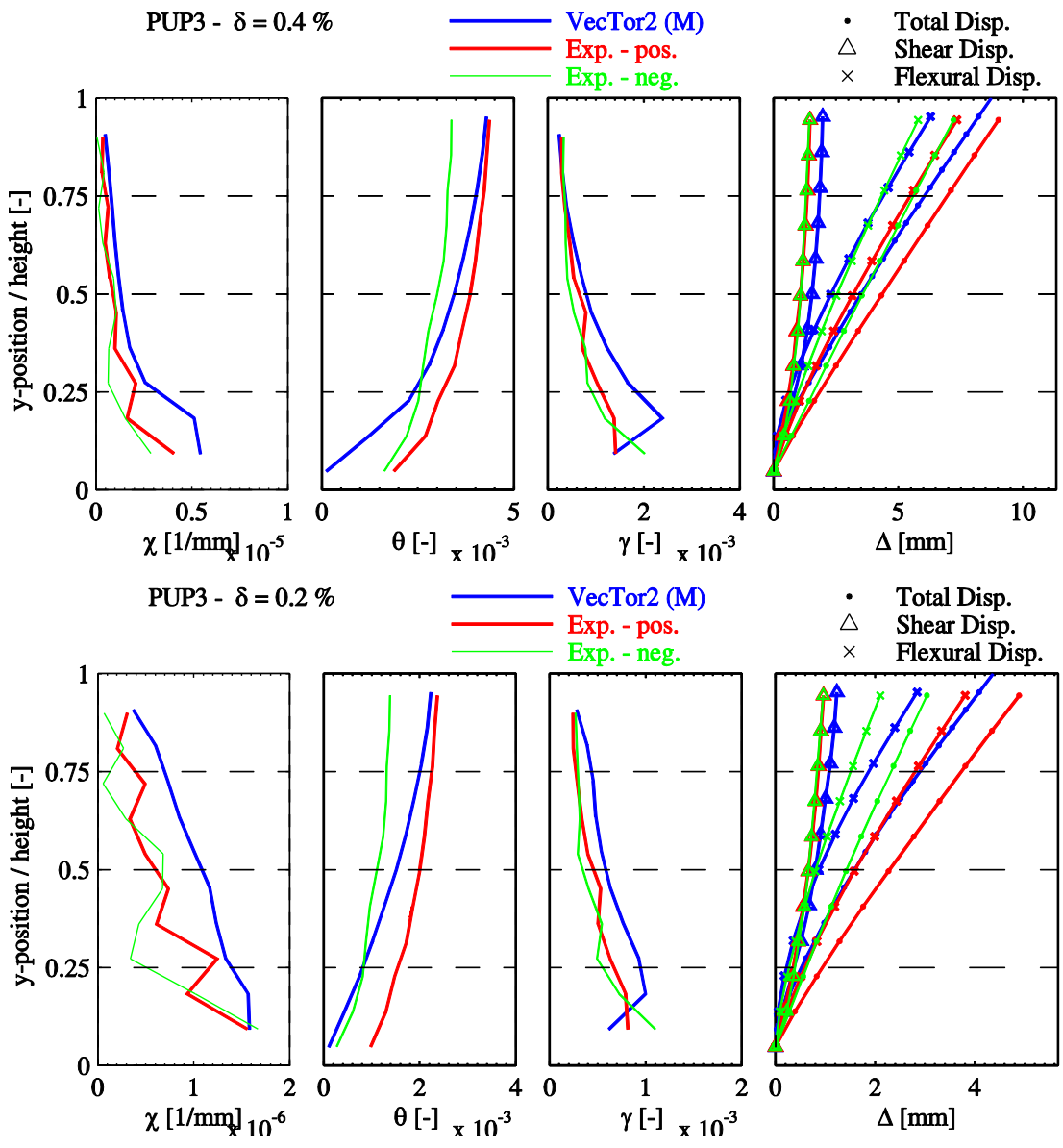

Figure 7. Comparison of deformation quantities of PUP3 for different drifts (a) 0.1 % and (b) 0.2 %

In Fig. 7 it can be observed that the DSFM tends to overestimate the curvature also for PUP3. Nevertheless, the differences are much lower than observed for PUP1. The shear span for PUP3 was significantly higher ($H_{0,PUP3}$ = 3 x $H_{0,PUP1}$) and thus the simplification of a continuous material done for the DSFM applies quite well. In previous section it was observed that the model in VecTor 2 underestimates the shear strains for small compression zones, while it overestimates when the whole section of the wall is in compression (see Fig. 5). This is now also reflected in the shear strain profiles over the height in Fig. 7. However, this mistake is compensated over the height and the similitude of the displacement components is satisfactory.

CONCLUSIONS

In this paper we use a newly published model based on the Disturbed Stress Field Model (DSFM), (Facconi et al., 2013) to model different unreinforced masonry walls which we tested at the laboratory of the EPF Lausanne, Switzerland. The model is based on the failure criterion developed by Ganz (1985) for unreinforced masonry (URM) walls and implemented in the software VecTor 2 (Wong et

al., 2013). Compared with conventional smeared crack models, the DSFM is able to combine the average macroscopic representation of the material behaviour with the local shear stress-shear slip response of mortar joints (Facconi et al., 2013).

In a first part of this article, we show that the use of DSFM gives good estimates of the initial stiffness but underestimates the displacement and force capacity of our URM walls composed of modern perforated clay bricks. During testing the walls were built on steel plates which confined the mortar joint at base and hindered thus to produce the typical tensile failure in brick-mortar interface at base (Petry and Beyer, 2014b). We show that this phenomenon can be accounted for by replacing the compression strength of the masonry in the first brick layer by the strength of the brick itself. Using this improved model, we compare the numerical results at the global and local level. We show that the simplification of the masonry to a continuous material is correct when regarding the global engineering demand parameters (EDPs), e.g., force-displacement behaviour of the walls. However, when comparing the local EDPs, e.g., curvature and rotation, significant differences can be obtained. These differences are mainly caused by the rotation of the bricks inside the walls (Mann and Müller, 1982). Through comparison of the local EDPs for a wall with a shorter shear span (H_0 = 0.5 H) and with a wall tested with a higher shear span (H_0 = 1.5 H), we show that the influence of the rotation gets less important with increasing shear span and that for a wall with higher shear span the assumption of continuous material can give reasonable results also at local level.

ACKNOWLEDGEMENTS

We thank Prof. Vecchio (University of Toronto) for sharing the VecTor 2 program with the implementation of the new model for unreinforced masonry walls.

REFERENCES

Facconi L, Plizzari G and Vecchio F (2013) "Disturbed Stress Field Model for Unreinforced Masonry," *Journal of Structural Engineering*, 10.1061/(ASCE)ST.1943-541X.0000906, 04013085

Gambarotta L and Lagomarsino S (1997) "Damage models for the seismic response of brick masonry shear walls. Part II: The continuum model and its applications," *Earthquake Engineering and Structural Dynamics*, 26: 441-462

Ganz HR (1985) Masonry walls subjected to normal and shear forces, Ph.D. Thesis, ETH Zurich, Switzerland (in German)

Lourenço PB (1996) Computational strategies for masonry structures, Ph.D. Thesis, Delft University of Technology, the Netherlands

Mann W and Müller H (1982) "Failure of Shear-Stressed Masonry - An Enlarged Theory, Tests and Application to Shear Walls," *In: Proc. of the British Ceramic Society* 1982; Vol. 30: 223-235

Pelà L, Cervera M and Roca P (2013) "An orthotropic damage model for the analysis of masonry structures," *Construction and Building Materials*, 41: 957-967

Petry S and Beyer K (2013) "Cyclic test data of six unreinforced masonry walls with different boundary conditions," *Submitted in Earthquake Spectra October 2013*

Petry S and Beyer K (2014a) "Influence of boundary conditions and size effect on the drift capacity of URM walls," *Engineering Structure*, 65: 76-88. DOI: 10.1016/j.engstruct.2014.01.048

Petry S and Beyer K (2014b) "Force-displacement relationship for in-plane loaded URM walls," *To be submitted*

Petry S and Beyer K (2014c) "Limit states of URM walls subjected to seismic in-plane loading," *Submitted to Bulletin of Earthquake Engineering February 2014*

SIA (2005) SIA 266: Masonry. Swiss code, Swiss Society of Engineers and Architects SIA, Zürich, Switzerland

Snozzi L and Molinari JF (2013) "A cohesive element model for mixed mode loading with frictional contact capabilities," *International Journal for Numerical Methods in Engineering*, 93(5): 510-526

Wong PS, Vecchio F and Trommels H (2013) "Vector2 & Formworks User's Manual," 2nd Ed.